

# Asymmetric Duffing oscillator: metamorphoses of 1 : 2 resonance and its interaction with the primary resonance

Jan Kyzioł, Andrzej Okniński  
Politechnika Świętokrzyska, Al. 1000-lecia PP 7,  
25-314 Kielce, Poland

July 19, 2024

## Abstract

We investigate the 1 : 2 resonance in the periodically forced asymmetric Duffing oscillator due to the period-doubling of the primary 1 : 1 resonance or forming independently, coexisting with the primary resonance. We compute the steady-state asymptotic solution – the amplitude-frequency implicit function. Working in the differential properties of implicit functions framework, we describe complicated metamorphoses of the 1 : 2 resonance and its interaction with the primary resonance.

## 1 Introduction and motivation

A period-doubling cascade of bifurcations is a typical route to chaos in nonlinear dynamical systems. A generic example is the asymmetric Duffing oscillator governed by the non-dimensional equation

$$\ddot{y} + 2\zeta\dot{y} + \gamma y^3 = F_0 + F \cos(\Omega t), \quad (1)$$

which has a single equilibrium and a corresponding one-well potential [1], where  $\zeta$ ,  $\gamma$ ,  $F_0$ ,  $F$  are parameters and  $\Omega$  is the angular frequency of the periodic force.

Szemplińska-Stupnicka elucidated the period-doubling scenario in the dynamical system (1) in a series of far-reaching papers [2–4]; see also [1] for a review and further results.

The main idea introduced in [2] consists of perturbing the main steady-state (approximate) asymptotic solution of Eq.(1)

$$y_0(t) = A_0 + A_1 \cos(\Omega t + \theta), \quad (2)$$

as

$$y(t) = y_0(t) + B \cos\left(\frac{1}{2}\Omega t + \varphi\right), \quad (3)$$

substituting  $y(t)$  into Eq.(1) and considering the condition  $B \neq 0$ . In papers [1–4], the authors found several conditions guaranteeing the formation and stability of solution (3) and used them to study the period-doubling phenomenon.

In our recent work, we studied the period-doubling scenariorising the period-doubling condition determined in [1–4] as an implicit function. More precisely, using the formalism of differential properties of implicit functions [5, 6], we derived analytic formulas for the birth of period-doubled solutions [7].

The motivation of this work stems from two observations: (i) in some cases, 1 : 2 resonance, coexisting with 1 : 1 resonance, is not created via the period doubling of 1 : 1 resonance, (ii) 1 : 2 resonance depends on the parameters in a more complicated way than the primary resonance.

Thus, the aim of the present work is to study metamorphoses of 1 : 2 resonance coexisting with the primary 1 : 1 resonance.

The paper is structured as follows: Section 2 describes amplitude-frequency curve for 1 : 2 resonance for Eq. (1). In Section 3, equations to compute singular points and vertical tangencies are derived. In Section 4, we present an example of metamorphoses of 1 : 2 resonance, based on computed singular points. In Section 5 we provide an example of similar metamorphoses for a different dynamical system, suggesting a greater generality of our results. We summarize our results in the last section.

## 2 The 1 : 2 resonance: steady-state solution

Since the 1 : 2 resonance can coexist, without contact, with the primary 1 : 1 resonance we assume the following steady-state solution of Eq.(1)

$$y(t) = B_0 + B \cos\left(\frac{1}{2}\Omega t + \varphi\right), \quad (4)$$

which can be computed proceeding as in [8, 9]. More exactly, we get

$$\frac{3}{2}\gamma B_0 B^2 + \gamma B_0^3 + \frac{3}{2}\gamma B_0 C^2 - F_0 + \frac{3}{4}\gamma B^2 C \cos 2\varphi = 0, \quad (5a)$$

$$\zeta B \Omega - 3\gamma B_0 B C \sin 2\varphi = 0, \quad (5b)$$

$$\frac{1}{4}B \Omega^2 - \frac{3}{4}\gamma B^3 - 3\gamma B_0^2 B - \frac{3}{2}\gamma B C^2 - 3\gamma B_0 B C \cos 2\varphi = 0, \quad (5c)$$

where

$$C = \frac{F}{\frac{3}{4}\gamma A^2 - \Omega^2}. \quad (5d)$$

We note that in papers [1, 2] a form describing a combination of 1 : 1 and 1 : 2 resonances was assumed (see Eq. (8.5.20) in [1] and Eq. (8a) in [2]) and thus different equations for the asymptotic solution were obtained.

Assuming  $B \neq 0$  we get from Eqs. (5b), (5c)

$$S_1(B_0, B, \Omega; \zeta, \gamma, F) = \zeta^2 \Omega^2 + \left(\frac{1}{4}\Omega^2 - \frac{3}{4}\gamma B^2 - 3\gamma B_0^2 - \frac{3}{2}\gamma C^2\right)^2 - 9\gamma^2 B_0^2 C^2 = 0, \quad (6)$$

Moreover, equations (5a) and (5c) lead to

$$S_2(B_0, B, \Omega; \zeta, \gamma, F_0, F) = \begin{aligned} & -B^2\Omega^2 + 3B^4\gamma - 12B^2\gamma B_0^2 + 6B^2\gamma C \\ & -16\gamma B_0^4 - 24\gamma B_0^2 C^2 + 16B_0 F_0 = 0. \end{aligned} \quad (7)$$

Equation (6) is quadratic concerning  $B_0^2$ . Therefore, we solve this equation for  $B_0^2$

$$B_0^2 = -\frac{1}{4}B^2 + \frac{1}{12\gamma}\Omega^2 \pm \frac{\sqrt{f(B, \Omega; \zeta, \gamma, F)}}{3\gamma(4\Omega^2 - 3\gamma B^2)^2} \quad (8)$$

$$f(B, \Omega; \zeta, \gamma, F) = -81\Omega^2\zeta^2\gamma^4 B^8 + 108\gamma^3(4\Omega^4\zeta^2 - 3F^2\gamma) B^6 - 108\Omega^2\gamma^2(8\Omega^4\zeta^2 - 9F^2\gamma) B^4 + 96\gamma\Omega^4(8\Omega^4\zeta^2 - 9F^2\gamma) B^2 - 256\zeta^2\Omega^{10} + 192F^2\gamma\Omega^6 - 576F^4\gamma^2$$

We substitute the following expression for  $B_0$

$$B_0(B, \Omega) = \sqrt{-\frac{1}{4}B^2 + \frac{1}{12\gamma}\Omega^2 - \frac{\sqrt{f(B, \Omega; \zeta, \gamma, F)}}{3\gamma(4\Omega^2 - 3\gamma B^2)^2}} \quad (9)$$

to Eq. (7) (it turns out that we have to choose the minus sign) to get a complicated but useful implicit non-polynomial function  $L(B, \Omega; \zeta, \gamma, F_0, F) = 0$

$$L(B, \Omega; \zeta, \gamma, F_0, F) = S_2(B_0(B, \Omega), B, \Omega; \zeta, \gamma, F_0, F). \quad (10)$$

### 3 Vertical tangencies and singular points

Equations for vertical tangencies read

$$L(B, \Omega; \zeta, \gamma, F_0, F) = 0, \quad (11a)$$

$$\frac{\partial L(B, \Omega; \zeta, \gamma, F_0, F)}{\partial B} = 0, \quad (11b)$$

while equations for singular points are

$$L(B, \Omega; \zeta, \gamma, F_0, F) = 0, \quad (12a)$$

$$\frac{\partial L(B, \Omega; \zeta, \gamma, F_0, F)}{\partial B} = 0, \quad (12b)$$

$$\frac{\partial L(B, \Omega; \zeta, \gamma, F_0, F)}{\partial \Omega} = 0. \quad (12c)$$

Equations (11), (12) can be solved numerically, yet simplify greatly for  $B = 0$ .

We check that  $[\partial L(B, \Omega; \zeta, \gamma, F_0, F) / \partial B]_{B=0}$ . Therefore, we obtain a simplified equation for vertical tangencies

$$L(0, \Omega; \zeta, \gamma, F_0, F) = 0. \quad (13)$$

Equation (13) can be solved for  $\Omega$  yielding

$$f_1(\Omega; \zeta, \gamma, F_0, F) = \Omega^{12} + 16\lambda^2\Omega^{10} - 12\gamma F^2\Omega^6 + 36\gamma^2 F^4 = 0, \quad (14a)$$

$$f_2(\Omega; \zeta, \gamma, F_0, F) = \sum_{k=0}^{18} a_k \Omega^{2k} = 0, \quad (14b)$$

where non-zero coefficients  $a_k$  are shown in Table 1.

Table 1: Non-zero coefficients  $a_k$  of the polynomial (14b)

$k$	$a_k$
18	1
17	$48\zeta^2$
16	$768\zeta^4$
15	$36\gamma F^2 - 3456\gamma F_0^2 + 4096\zeta^6$
14	$1152\zeta^2\gamma F^2 + 165\,888\zeta^2\gamma F_0^2$
13	$9216\gamma F^2\zeta^4$
12	$756\gamma^2 F^4 - 248\,832\gamma^2 F^2 F_0^2 + 2985\,984\gamma^2 F_0^4$
11	$24\,192\zeta^2\gamma^2 F^4 + 1990\,656\gamma^2 F^2 F_0^2\zeta^2$
10	$193\,536\gamma^2 F^4\zeta^4$
9	$3456\gamma^3 F^6 - 2239\,488\gamma^3 F^4 F_0^2$
8	$165\,888\gamma^3 F^6\zeta^2$
6	$-31\,104\gamma^4 F^8 + 4478\,976\gamma^4 F_0^2 F^6$
5	$2488\,320\gamma^4 F^8\zeta^2$
3	$-933\,120F^{10}\gamma^5$
0	$4665\,600F^{12}\gamma^6$

Moreover, equation for singular points (12) in the case  $B = 0$  can be significantly simplified, demanding that the equation (14b) has a double root (equation (14a) has no physical double roots). We can request that the discriminant of the polynomial  $f_2(\Omega)$  vanishes or solve the equivalent set of equations

$$f_2(\Omega; \zeta, \gamma, F_0, F) = 0, \quad (15a)$$

$$\frac{\partial f_2(\Omega; \zeta, \gamma, F_0, F)}{\partial \Omega} = 0. \quad (15b)$$

By solving Eqs. (15) for  $F_0, F$  we obtain clear and simplified equations for singular points, making the computations easier,

$$p(Z) = d_{12}Z^{12} + d_{10}Z^{10} + d_8Z^8 + d_6Z^6 + d_4Z^4 + d_2Z^2 + d_0 = 0, \quad (16)$$

$$\begin{aligned} d_{12} &= 466\,560\gamma^6, \quad d_{10} = -233\,280\gamma^5\Omega^2, \quad d_8 = 20\,736\gamma^4\Omega^2(2\Omega^2 + 11\zeta^2), \\ d_6 &= -1728\gamma^3\Omega^4(2\Omega^2 + 41\zeta^2), \quad d_4 = 54\gamma^2\Omega^4(3\Omega^4 + 112\zeta^2\Omega^2 + 448\zeta^4), \\ d_2 &= -3\gamma\Omega^6\Omega^4 + 72\zeta^2\Omega^2 + 896\zeta^4, \quad d_0 = 4\zeta^2\Omega^6(\Omega^4 + 20\zeta^2\Omega^2 + 64\zeta^4). \end{aligned}$$

where  $Z = \frac{F}{\Omega^2}$ , and

$$q(T) = e_2 T^2 + e_0 = 0, \quad (17)$$

$$\begin{aligned} e_2 &= 1728\gamma\Omega^6 + 41472\gamma\zeta^2\Omega^4 + 1603584\gamma\zeta^4\Omega^2 + 22118400\gamma\zeta^6, \\ e_0 &= -\Omega^{14} + (-534Z^2\gamma + 592\zeta^2)\Omega^{12} + \left( \begin{array}{c} 15768Z^4\gamma^2 - 31968Z^2\zeta^2\gamma \\ +20128\zeta^4 \end{array} \right)\Omega^{10} \\ &+ (-247968Z^6\gamma^3 + 627552Z^4\zeta^2\gamma^2 - 499008Z^2\zeta^4\gamma + 195072\zeta^6)\Omega^8 \\ &+ \left( \begin{array}{c} 1736640Z^8\gamma^4 - 3805056Z^6\zeta^2\gamma^3 + 2596608Z^4\zeta^4\gamma^2 \\ -958464Z^2\zeta^6\gamma + 458752\zeta^8 \end{array} \right)\Omega^6 \\ &+ \left( \begin{array}{c} -4199040Z^{10}\gamma^5 + 9642240Z^8\zeta^2\gamma^4 + 7617024Z^6\zeta^4\gamma^3 \\ -40255488Z^4\zeta^6\gamma^2 + 16465920Z^2\zeta^8\gamma \end{array} \right)\Omega^4 \\ &+ (-19906560Z^{10}\zeta^2\gamma^5 - 76308480Z^8\zeta^4\gamma^4 + 23224320Z^6\zeta^6\gamma^3)\Omega^2 \\ &- 99532800Z^{10}\zeta^4\gamma^5. \end{aligned}$$

where  $T = F_0\Omega$ .

## 4 Numerical verification

In this Section, we shall compute singular points as well as vertical tangencies for chosen values of  $\zeta$ ,  $\gamma$ , and  $\Omega$ . In the case  $B = 0$ , we use Eqs. (15) in reduced form (16) and (17) to compute singular points and Eqs. (14) to compute vertical tangencies. Then, in the case  $B \neq 0$ , we use Eqs. (12) and (11), respectively.

In what follows we choose for  $B = 0$ , quite arbitrarily,  $\zeta = 0.09$ ,  $\gamma = 0.3$ ,  $\Omega = 1.5$ .

### 4.1 Singular points and vertical tangencies, $B = 0$

Thus, the singular point is chosen as  $(B, \Omega) = (0, 1.5)$ . We need to compute the parameters,  $F_0$  and  $F$ , for which the selected point is singular.

Therefore, for  $\zeta = 0.09$ ,  $\gamma = 0.3$ ,  $\Omega = 1.5$ , and  $B = 0$ , we solve equation  $p(Z) = 0$ , with  $p(Z)$  defined in Eq. (16), obtaining four positive roots,  $Z = 0.198445, 0.509084, 1.095980, 1.259811$ . We check, however, that only  $Z = 1.095980$  leads to a solution of (12). Since  $Z = F/\Omega^2$ , we get, for  $Z = 1.095980$ ,  $F = 2.465955$ . We now solve  $q(T) = 0$ , with  $q(T)$  defined in Eq. (17), obtaining for  $Z = 1.095980$  one positive root  $T = 0.112203$ . Since  $T = F_0\Omega$  we get  $F_0 = 0.074802$ .

Now, we check that for  $\gamma = 0.3$ ,  $F_0 = 0.074802$ ,  $F = 2.465955$  equations (12), solved numerically, yield indeed  $\zeta = 0.09$  and an isolated singular point  $(B, \Omega) = (0, 1.5)$ , see Fig. 1.

To find vertical tangencies, we set, for example,  $\zeta = 0.082$  and use just computed parameter values:  $\gamma = 0.3$ ,  $F_0 = 0.074802$ ,  $F = 2.465955$ . Solving equation (14b), we get  $(B, \Omega) = (0, 1.474612), (0, 1.527914)$  (all solutions of Eq. (14a are complex); see red boxes in Fig. 1.

## 4.2 Singular points and vertical tangencies, $B \neq 0$

We work with parameter values computed in the preceding subsection, i.e.,  $\gamma = 0.3$ ,  $F_0 = 0.074802$ ,  $F = 2.465955$ . We have shown in the prior Section that equations (12) have for  $\zeta = 0.09$  an isolated singular point  $(B, \Omega) = (0, 1.5)$ .

Moreover, equations (12) have other singular points for  $\gamma = 0.3$ ,  $F_0 = 0.074802$ ,  $F = 2.465955$ , and  $B \neq 0$ . Solving numerically Eqs. (12) we get (i)  $\zeta = 0.086504$  and a pair of self-intersections  $(B, \Omega) = (\pm 0.305755, 1.496498)$ , (ii) a pair of isolated points,  $\zeta = 0.108010$ ,  $(B, \Omega) = (\pm 1.069257, 1.613277)$ , see Fig. 1 where we show all singular points.

We also compute vertical tangencies for  $B \neq 0$ . Solving equations (11a) and (11b) numerically for  $\gamma, F_0, F$  listed above and  $\zeta = 0.082$  we get  $(B, \Omega) = (\pm 0.318833, 1.514052)$ ; see red boxes in Fig. 1.

## 4.3 Amplitude-frequency plots and bifurcation diagrams

We can show all singular points computed for 1 : 2 resonance in one plot.

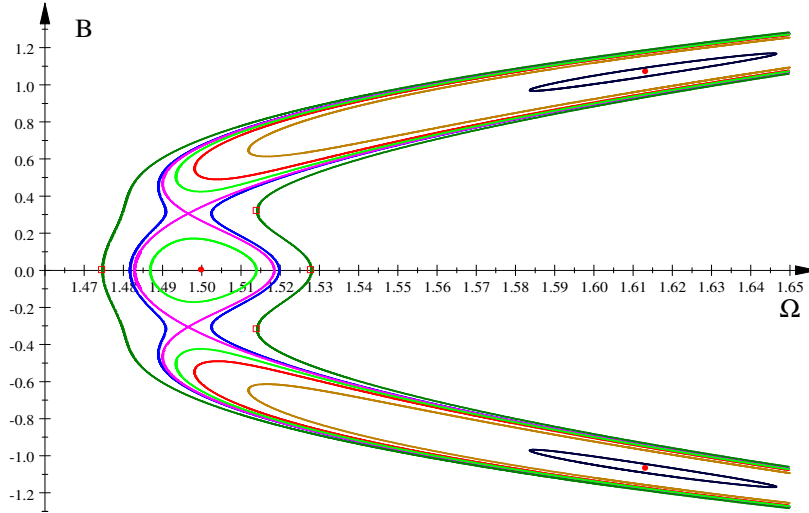


Figure 1: Sequential metamorphoses of amplitude-frequency implicit function  $L(B, \Omega; \zeta, \gamma, F_0, F) = 0$ , describing 1 : 2 resonance.

Parameters in Fig. 1 are  $\gamma = 0.3$ ,  $F_0 = 0.07480195$ ,  $F = 2.465954$ , and  $\zeta = 0.108010$  (two red dots), 0.1072 (navy), 0.095 (sienna), 0.09 (red, a dot and two branches), 0.088 (light green, an oval and two branches), 0.086504 (magenta, two self-intersections), 0.086 (blue), 0.082 (green).

We have computed bifurcation diagrams solving Eq. (1) numerically – obtaining  $y(t)$  as a function of  $\Omega$ ; see figures below. Comparison with Fig. 1 reveals which branches are stable. Colors in bifurcation diagrams correspond to those in Fig. 1. We thus document metamorphoses of 1 : 2 resonance (two

branches, colored) and its interaction with the primary 1 : 1 resonance (one branch in the middle, black).

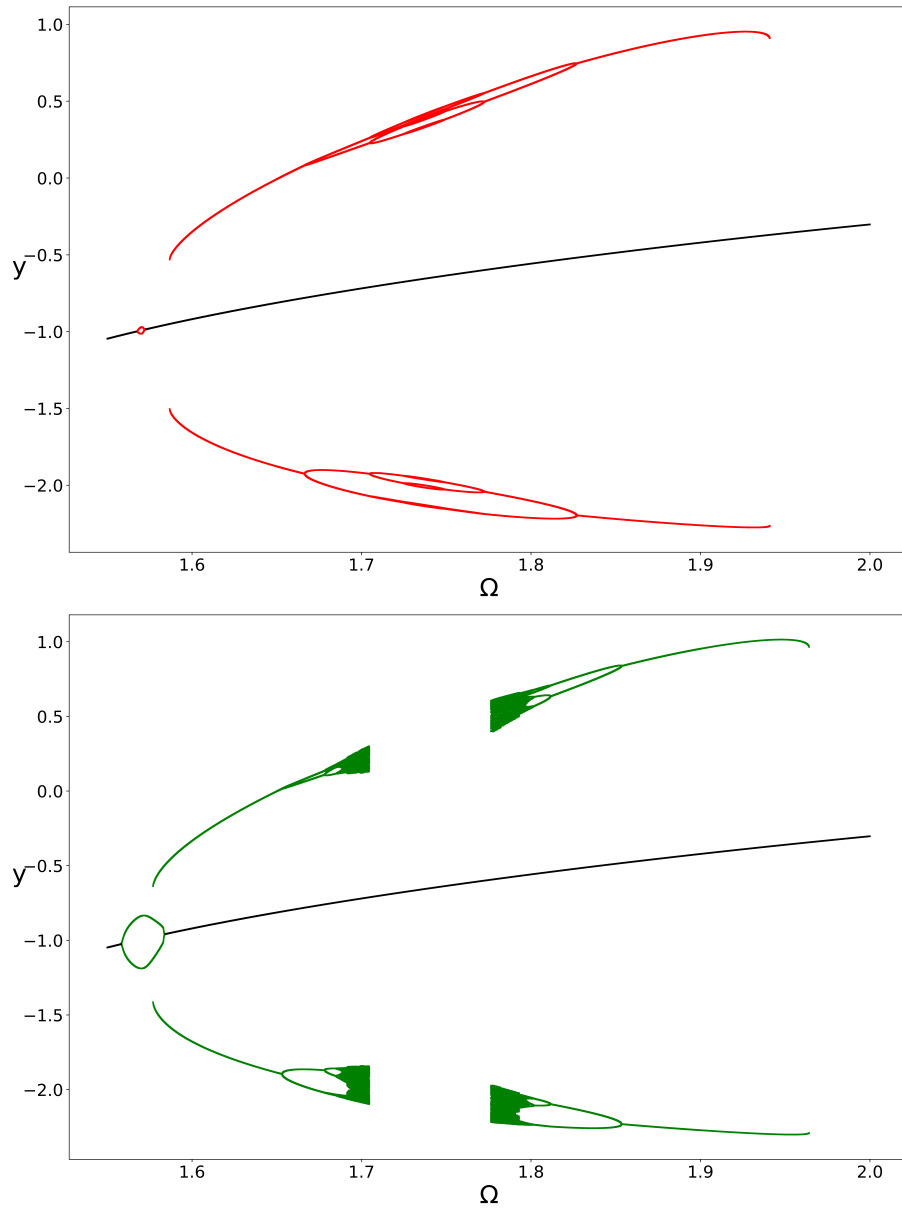


Figure 2: Bifurcation diagrams,  $\zeta = 0.094185$  (top),  $\zeta = 0.091$  (bottom).

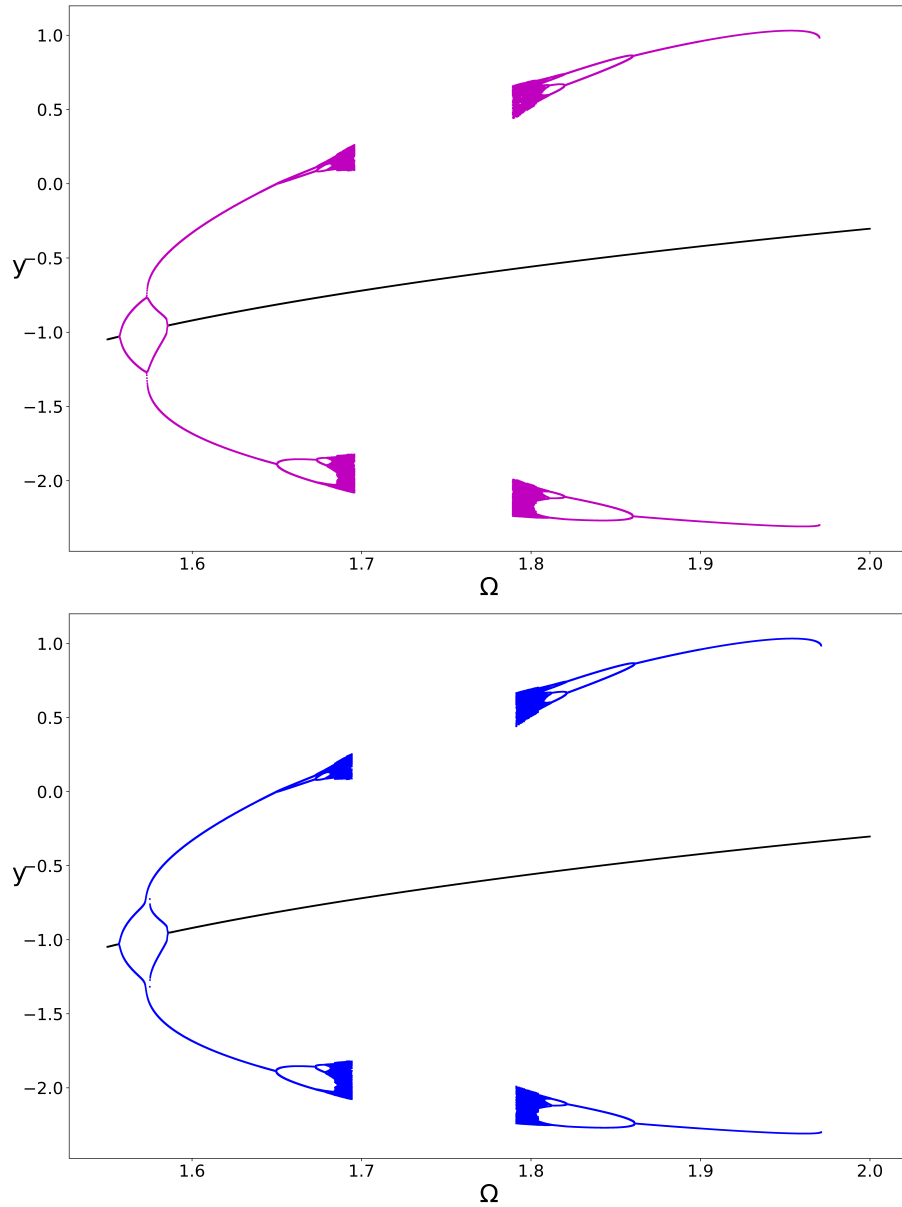


Figure 3: Bifurcation diagrams,  $\zeta = 0.09014$  (top),  $\zeta = 0.90$  (bottom).

#### 4.4 Description of transmutations of 1 : 2 resonance

We describe metamorphoses of 1 : 2 resonance for  $\gamma = 0.3$ ,  $F_0 = 0.074802$ ,  $F = 2.465955$  and descending values of  $\zeta$ . In what follows,  $\zeta_n$  denotes values



of  $\zeta$  computed integrating numerically the Duffing equation (1) while  $\zeta_a$  means values of  $\zeta$  computed from analytical condition (12) for singular points. We have computed function  $L(B, \Omega; \zeta, \gamma, F_0, F)$  from the asymptotic solution (4) and (5).

In Fig. 1, transmutations of function  $L(B, \Omega; \zeta, \gamma, F_0, F)$  are shown, and in bifurcation diagrams 2 and 3, metamorphoses of solutions of Duffing equation (1), are presented. We note good qualitative correspondence between predicted transmutations shown in Fig. 1 and metamorphoses of the solutions of the Duffing equation documented in Figs. 2 and 3.

We describe these changes as follows.

1. For  $\zeta_n = 0.11469$  ( $\zeta_a = 0.108010$ ), 1 : 2 resonance appears for the first time at  $\Omega_n = 1.722$  ( $\Omega_a = 1.613$ ); see two red dots (singular isolated points) in Fig. 1 (we do not show the corresponding bifurcation diagrams). For descending values of  $\zeta$ , the 1 : 2 resonance grows and transforms rapidly. More precisely, two inverted cascades form, then break and pull out – we discuss these changes in Section 5.
2. For  $\zeta_n = 0.094185$  ( $\zeta_a = 0.09$ ), a new isolated point of 1 : 2 resonance (red) appears on 1 : 1 resonance (black) at  $\Omega_n = 1.57$  ( $\Omega_a = 1.5$ ); see small red circle in top figure 2 or red dot in Fig. 1. The primary 1 : 1 resonance is black.

It is the first contact of these resonances. [Note that the 1 : 2 resonance has been subject to two-period doublings but has not broken yet.]

3. The singular, isolated point gives rise to an oval – a period- doubling of 1 : 1 resonance; see the light green line in Fig. 1 and green oval in bottom figure 2. The 1 : 1 resonance is black.

There is still no contact between the primer 1 : 2 resonance and the primary resonance [there are already two whole cascades of period-doublings of 1 : 2 resonance that have been disrupted and moved away; we call them left and right; see green lines in Fig. 2)].

4. For  $\zeta_n = 0.09014$  ( $\zeta_a = 0.086504$ ), there are two self-intersections (two singular points) at  $\Omega_n = 1.573$  ( $\Omega_a = 1.496$ ) and resonance 1 : 1 and left resonance 1 : 2 merge, see magenta lines in Fig. 1 and top figure 3. The right 1 : 2 resonance stays separated. The primary resonance is black.
5. For  $\zeta < \zeta_n = 0.09014$  ( $\zeta_a < 0.086504$ ), connected branches split another way; see blue lines in Fig. 1 and Fig. 3. The primary 1 : 1 resonance (black) absorbs the left 1 : 2 resonance with the whole cascade of period doublings, there is also another branch of 1 : 1 resonance, with one period doubling. The right 1 : 2 resonance stays unchanged.

Summing up, the separate 1 : 2 resonance, after the first contact with 1 : 1 resonance, splits into two parts, left and right, then the left resonance 1 : 2 merges with the primary 1 : 1 resonance and splits another way, while the right 1 : 2 resonance does not evolve.

## 5 On the formation of period-doubling cascades and their subsequent breaking

In the preceding section, we described complicated interactions of 1 : 2 and 1 : 1 resonances, which are generic for dynamical system 1. We thus decided to investigate the generality of our scenario by computing bifurcation diagrams for another resonance in another dynamical system.

More precisely, we analyzed a vibrating system with two minima of potential energy, studied by Szemplińska-Stupnicka

$$\frac{d^2x}{dt^2} + h\frac{dx}{dt} - \frac{1}{2}x + \frac{1}{2}x^3 = F \cos(\omega t), \quad (18)$$

see Eq. (4.2) in [10]. We computed bifurcation diagrams for the 1 : 1 resonance

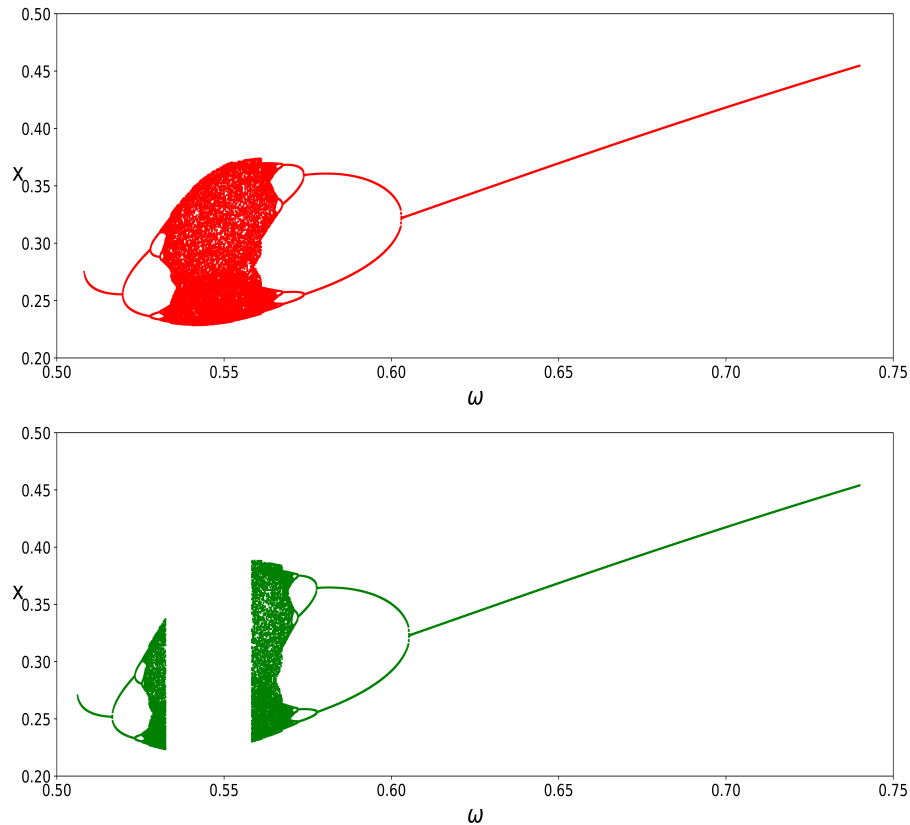


Figure 4: Bifurcation diagrams for Eq. (18),  $F = 0.0620, h = 0.1259$  (red, top),  $F = 0.0620, h = 0.1258$  (green, bottom).

of Eq. (18) for  $F = 0.0620, h = 0.1259$  (red), and  $F = 0.0620, h = 0.1259$  (green).

We see that fully developed cascade breaks in close analogy to transformation shown in Fig. 2 for the 1 : 2 resonance. We attribute disruption of the cascade to crisis, cf. comments below Fig. 4.15 in [10] (it seems that for  $h = 0.1$  the second cascade was destroyed completely).

It seems typical to break a fully developed cascade by forming two cascades. Note that in this case, one of these cascades may remain unnoticed.

## 6 Summary and most important findings

Based on the amplitude-frequency steady-state implicit equation (10) computed for Eq. (1), we studied the metamorphoses of the resonance 1 : 2 and its interaction with the primary resonance 1 : 1.

Working in the formalism of differential properties of implicit functions, we derived formulas to compute singular points of the amplitude-frequency function  $L(B, \Omega; \zeta, \gamma, F_0, F)$ , defined in (10); see Section 3. It should be stressed that the dynamics of the initial equation (1) change in the neighborhood of singular points (in the parameter space).

In Section 4, after choosing arbitrary parameters  $\zeta = 0.09$ ,  $\gamma = 0.3$ ,  $\Omega = 1.5$ , and  $B = 0$ , we (i) first solved Eqs. (15), (17) obtaining  $F = 2.465955$ ,  $F_0 = 0.074802$ . We thus (ii) computed parameters of the singular point  $(B, \Omega) = (0, 1.5)$ ; see red dot in Fig. 1. Other singular points were computed numerically from Eqs. (12). See two magenta self-intersections and two red dots in Fig. 1.

Working in this order is relatively easy as we know the position of the first singular point  $(B, \Omega) = (0, 1.5)$ ; thus two other pairs of singular points should not be too far away on the  $\Omega$  axis. This information is of great help in solving Eqs. (12) numerically.

We also computed bifurcation diagrams solving Eq. (1) numerically, shown in Figs. 2 and 3, obtaining good agreement with the amplitude-frequency profiles of Fig. 1. Subsection 4.4 provides a detailed description of metamorphoses of 1 : 2 resonance. Section 5 shows another example of cascade disruption.

The most significant achievements of this work, consisting of computing singular points of the amplitude-frequency implicit function (10), are

1. The semi-analytic procedure to compute singular, isolated points of 1 : 2 resonance, consisting of Eqs. (16) and (17). These points correspond to the first contact of resonances 1 : 2 and 1 : 1.  
Numerical computation of a pair of isolated points that indicate the birth of 1 : 2 resonance.
2. Discovery and detailed description of complicated transmutations of 1 : 2 resonance that resulted in the first contact with the primary 1 : 1 resonance, disruption of the 1 : 2 resonance into two parts, left and right, merging of the left 1 : 2 resonance with the primary 1 : 1 resonance, and breaking again; the right 1 : 2 resonance effectively not evolving.
3. Discovery of analogous metamorphoses in a different dynamical system, suggesting a greater generality of our results; see Section 5.

## A Computational details

Nonlinear equations were solved numerically using the computational engine Maple 4.0 from Scientific WorkPlace 4.0.

Figure 1 was plotted with the computational engine MuPAD 4.0 from Scientific WorkPlace 5.5. Bifurcation diagrams in Figs. 2, 3, and 4 were computed by integrating numerically Eq. (1) running DYNAMICS [11] as well as our programs written in Pascal and Python [12].

## References

- [1] I. Kovacic, M.J. Brennan. Forced harmonic vibration of an asymmetric Duffing oscillator. In: *The Duffing Equation: Nonlinear Oscillators and Their Behavior*. (Eds.: I. Kovacic, M.J. Brennan). John Wiley & Sons, Hoboken, New Jersey 2011; pp. 277 - 322.
- [2] W. Szemplińska-Stupnicka, J. Bajkowski, The 1/2 subharmonic resonance and its transition to chaotic motion in a non-linear oscillator, *Int. J. Nonlinear Mech.* **21** (1986) 401-419.
- [3] W. Szemplińska-Stupnicka, Secondary resonances and approximate models of routes to chaotic motion in non-linear oscillators, *J. Sound and Vibration* **113** (1987) 155-172.
- [4] W. Szemplińska-Stupnicka, Bifurcations of harmonic solution leading to chaotic motion in the softening type Duffing's oscillator, *Int. J. Nonlinear Mech.* **23** (1988) 257-277.
- [5] G.M. Fikhtengol'ts, (I.N Sneddon, Editor) *The fundamentals of mathematical analysis*, Vol. 2, Elsevier, 2014 (Chapter 19), translated from Russian, Moscow, 1969.
- [6] J. Kyzioł, A. Okniński. Localizing bifurcations in nonlinear dynamical systems via analytical and numerical methods, *Processes* **10** (2022) 127, 17 pages.
- [7] J. Kyzioł, A. Okniński. Asymmetric Duffing oscillator: the birth and build-up of period doubling, *arXiv*: 2312.00830 [nlin.CD].
- [8] K.L. Janicki, W. Szemplińska-Stupnicka. SUBHARMONIC RESONANCES AND CRITERIA FOR ESCAPE AND CHAOS IN A DRIVEN OSCILLATOR, *Journal of Sound and Vibration* **180** (1995) 253-269.
- [9] K.L. Janicki. PhD Thesis (in Polish), Institute of Fundamental Technological Research PAS, 16/1994, <https://rcin.org.pl/dlibra/doccontent?id=686f>.
- [10] W. Szemplińska-Stupnicka. *Chaos, Bifurcations and Fractals Around Us: A Brief Introduction*. Vol. 47. World Scientific, 2003.

- [11] Nusse, Helena E., James A. Yorke. *Dynamics: numerical explorations: accompanying computer program dynamics*. Vol. 101. Springer, 2012.
- [12] Fernando Pérez, Brian E. Granger, IPython, *A System for Interactive Scientific Computing*, *Computing in Science and Engineering*, vol. 9, no. 3, pp. 21-29, May/June 2007, doi:10.1109/MCSE.2007.53. URL: <https://ipython.org>